Spectrochimica Acta Part A: Molecular and Biomolecular Spectroscopy 101 (2013) 91–99

Contents lists available at SciVerse ScienceDirect

Spectrochimica Acta Part A: Molecular and Biomolecular Spectroscopy

journal homepage: www.elsevier.com/locate/saa

FT-IR, FT-Raman spectral and conformational studies on (*E*)-2-(2-hydroxybenzylidenamino)-3-(1H-indol-3yl) propionic acid

H. Saleem [a], S. Subashchandrabose [b,*], Y. Erdogdu [c], V. Thanikachalam [d], J. Jayabharathi [d]

[a] Dept. of Physics, Annamalai University, Annamalai Nagar, Tamil Nadu 608 002, India
[b] Dept. of Physics, M.A.R. College of Engg. and Tech., Trichy, Tamil Nadu 621 316, India
[c] Dept. of Physics, Ahi Evran University, Kirsehir 40040, Turkey
[d] Dept. of Chemistry, Annamalai University, Annamalai Nagar, Tamil Nadu 608 002, India

HIGHLIGHTS

- Structural properties of (*E*)-2HBA3IPA.
- Detailed vibrational assignments using TED.
- Intra-molecular charge transfer calculations.
- Hyperpolarizability calculation.
- Band gap energy.

GRAPHICAL ABSTRACT

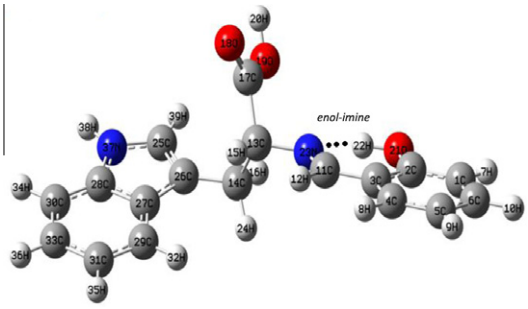

ARTICLE INFO

Article history:
Received 12 June 2012
Received in revised form 30 August 2012
Accepted 9 September 2012
Available online 16 September 2012

Keywords:
FT-IR
FT-Raman
TED
NBO
(*E*)-2HBA3IPA)

ABSTRACT

The (*E*)-2-(2-hydroxybenzylidenamino)-3-(1H-indol-3yl) propionic acid ((*E*)-2HBA3IPA) was synthesized. The theoretical conformational analysis was performed to identify the stable structure. Optimized molecular bond parameters were calculated by using B3LYP/6-31G(d,p) basis set. The hyperconjugative interaction energy ($E^{(2)}$) and electron densities of donor (i) and acceptor (j) bonds were calculated using NBO analysis. First order hyperpolarizability (β_0) was calculated. The band gap energy was analyzed by UV–Visible recorded spectra and compared with theoretical band gap TD-DFT/B3LYP/6-31G(d,p) values. The intra-molecular hydrogen bonding interaction was identified between nitrogen and hydroxyl hydrogen (N···H—O).

Introduction

Some Schiff bases which are derived from salicylaldehyde have attracted the interest of chemists and physicists because they show thermochromism and photochromism in the solid state by proton atom transfer from the hydroxyl oxygen atom to the nitrogen atom [1]. Indole is an aromatic heterocyclic organic compound with a bicyclic structure, it consist of a six-member benzene ring fused to five-member nitrogen containing pyrrole ring. It is of interest as it can be compare with tryptophane residue [2]. The derivative of indole is present in both-animal and plants. The most important compound of this group is tryptophan, an essential amino acid in the human diet, which is a 3-substituted indole [3]. Another important indole derivative is the indole-3acetic acid, a phytohormone, coordinating several growing processes of plants [4]. The biological activity of the indole derivatives is in connection with the nature of substitution in positions 3, on the pyrrole ring [5]. Indole derivatives have an important role through individual biological functions. It is present in the side chain of amino acid tryptophan. The chemical and spectroscopic properties of indole

* Corresponding author. Mobile +91 9976853476.
E-mail addresses: saleem_h2001@yahoo.com (H. Saleem), sscbphysics@gmail.com (S. Subashchandrabose).

1386-1425/$ - see front matter © 2012 Elsevier B.V. All rights reserved.
http://dx.doi.org/10.1016/j.saa.2012.09.023

derivatives have been subject of many experimental and theoretical investigations [6]. The pineal indole, namely 5-methoxy tryptamine, one of the biogenic monoamines, would play anti-tumor effects, by either inhibiting cancer cell proliferation or stimulating the anticancer immunity [7].

Literature survey reveals that to the best of our knowledge neither the complete IR and Raman spectra nor the force field for (*E*)-2HBA3IPA have been reported so for. Therefore the present investigation was undertaken to study the vibrational spectra of the title molecule completely and to identify the various modes with greater wavenumber accuracy. The *ab initio* DFT calculation has been performed to support our wavenumber assignments, conformational analysis, bond parameters, hyperpolarizability calculation; NBO and HOMO–LUMO band gap have also been studied.

Experimental

Synthesis

The compound (*E*)-2HBA3IPA was synthesized by mixing the salicylaldehyde in ethanol and sodium salt of tryptophan in ethanol–water (50%v/v) Howard et al. [8]. The mixture was heated and refluxed on a mantel about 5 h. The reaction mixture was cooled to room temperature and neutralized by 1:1 HCl. The white Schiff base was separated, filtered off, washed thoroughly with deionised water ethanol mixture followed by ether wash. The product obtained was dried over vacuum desiccators. The melting point of the compound is 114 °C (lit 114 °C) [8].

FT-Raman and FT-IR spectra

The FT-Raman spectrum of (*E*)-2HBA3IPA was recorded using the 1064 nm line of a Nd:YAG laser as excitation wavelength in the region 50–3500 cm^{-1} on a Bruker model IFS 66 V spectrophotometer equipped with an FRA 106 FT-Raman module accessory. The spectral measurements were carried out at Sree Chitra Tirunal Institute for Medical Sciences and Technology, Poojappura, Thiruvananthapuram, Kerala, India. The FT-IR spectrum of this compound was recorded in the region 400–4000 cm^{-1} on an IFS 66 V spectrophotometer using the KBr pellet technique. The spectrum was recorded at room temperature, with a scanning speed of 10 cm^{-1} per minute and at the spectral resolution of 2.0 cm^{-1} in CISL Laboratory, Annamalai University, Tamilnadu, India.

Computational details

The entire calculations were performed at DFT levels on a Pentium 1 V/3.02 GHz personal computer using Gaussian 03W [9] program package, invoking gradient geometry optimization [9,10]. Initial geometry generated from standard geometrical parameters was minimized without any constraint in the potential energy surface at DFT level, adopting the standard 6-31G(d,p) basis set. The optimized structural parameters were used in the vibrational frequency calculations at the DFT level to characterize all stationary points as minima. Then, vibrationally averaged nuclear positions of (*E*)-2HBA3IPA were used for harmonic vibrational frequency calculations resulting in IR and Raman frequencies together with intensities and Raman depolarization ratios. In this study, the DFT method B3LYP/6-31G(d,p) was used for the computation of molecular structure, vibrational frequencies and energies of optimized structures. The vibrational modes were assigned on the basis of TED analysis using SQM program [11].

It should be noted that Gaussian 03W package able to calculate the Raman activity. The Raman activities were transformed into Raman intensities using Raint program [12] by the expression:

$$I_i = 10^{-12} \times (v_0 - v_i)^4 \times \frac{1}{v_i} \times \mathrm{RA}_i \quad (1)$$

where I_i is the Raman intensity, RA_i is the Raman scattering activities, v_i is the wavenumber of the normal modes and v_0 denotes the wavenumber of the excitation laser [13].

Results and discussion

Molecular geometric

The optimized structure of (*E*)-2HBA3IPA is calculated at B3LYP/6-31G(d,p) level of theory. To find stable conformer, a meticulous conformational analysis was carried out for the title compound. A selected dihedral angle was rotated by 10 degree intervals around the free rotation bonds, conformational space of the title compound was scanned by molecular mechanic simulations and then full geometry optimizations of these structures were performed by B3LYP/6-31G(d,p) method. Results of geometry optimizations were indicated that the title compound is rather flexible molecule and, in theory, may have at least twenty-eight conformers as shown in Fig. S1 (Supplementary). Ground state energies, zero point corrected energies ($E_{\mathrm{elect.}}$ + ZPE), relative energies and dipole moments of conformers were presented in Table S1 (Supplementary). Zero point corrections have not caused any significant changes in the stability order.

The bond parameters were calculated for enol–imine closed (real molecule) form and open (isolated molecule gas phase) form. The enol–imine closed form is more stable. Salicylideneanile is an aromatic Schiff base, which has long-ranged π-electron delocalization capacity during the proton transfer reaction, O—H···N ↔ O···H—N [14,15]. The similar trend has been observed in our present work. Due to the π-electron donation from nitrogen to salicylidene ring, bond lengths, bond angles and dihedral angles are distorted from the stable structure. In this regard, C—O and C—N bonds are the most sensitive indicators [16]. From our investigation, the bond length of C2—O21 is about 1.340 Å is in closed form (enol-hydrogen bonding), whereas the same bond is calculated about 1.356 Å when the hydrogen is outwards to the nitrogen. Similarly the calculated C11—N23 bond lengths are 1.288 and 1.277 Å for enol imine closed and enol imine open form, respectively. The intra-molecular hydrogen bonding between nitrogen and hydrogen (O_{21}—H_{22}···N_{23}) atom is calculated about 1.725 Å, which is in consistent with literature values [17–19]. The bond lengths C_1—C_2 (1.404), C_5—C_6 (1.404) are positively deviated from the C—C values calculated by enol open form. These values are supported by Wang et al. [19]. Literature survey reveals that the C—O bond lengths in the carboxylic acid group of 5-flourosalicylic acid are 1.225 Å (C=O) and 1.308 Å (C—O) [20]. In this study the calculated bond length C_{17}=O_{18} (1.209 Å) and C_{17}—O_{19} (1.355 Å) are in line with the literature values. The enol open form is shown in Fig. S2 (Supplementary).

To the best of our knowledge no X-ray crystallographic data of this molecule has been established. However, the theoretical results obtained are almost comparable with the molecule. For the title compound, the bond angles C_{17}—O_{19}—H_{20} = 105.92° and C_2—O_{21}—H_{22} = 107.39° of the C—O—H group, which are differ by 1.47°. This may be due to the formation of intra-molecular hydrogen bond (O_{21}—H_{22}···N_{23}). The shortening of bond distance of C_{11}—N_{23}/1.288 Å is due to the delocalization of π-electron during the formation of intra-molecular hydrogen bond, while the bond distance for C_{13}—N_{23} is 1.457 Å. The dihedral angles O_{18}—C_{17}—O_{19}—H_{20} = 1.34° (carboxylic group) and C_3—C_{11}—N_{23}—C_{13} = 179.85°, which confirms *cis* and *trans* form respectively. The bond parameters of indole (tryptophan) in the present molecule are in

agreement with values [4]. The optimized structure is shown in Fig. 1 and bond parameters are listed in Table S2 (Supplementary).

Vibrational assignments

The compound (*E*)-2HBA3IPA was synthesized, it consist 39 atoms and hence 111 normal modes of vibrations. This molecule belongs to C_1 point group symmetry. The fundamental vibrational wavenumbers of (*E*)-2HBA3IPA calculated by DFT (B3LYP/6-31G (d,p)) method. The calculated wavenumbers are given in Table 1. The resulting vibrational wavenumbers for the optimized geometries, IR intensities as well as Raman scattering activities and experimental FT-IR, FT-Raman frequencies are also listed. A combined experimental and theoretical spectrum of title compound has been shown in Fig. 2 (FT-IR) and Fig. 3 (FT-Raman). The normal modes of vibration were assigned on the basis of TED. To bring the theoretical values closer to experimental values, we used the scale factor: 0.9608 [21].

N—H vibrations

The N—H stretching vibrations occur in the region 3300–3500 cm^{-1} [22]. The hetero aromatic molecule containing N—H group shows its stretching absorption in the region 3500–3220 cm^{-1} [23]. Pyrroles, indols and carbazole in non-polar compounds display very strong N—H stretching absorption between 3500 and 3450 cm^{-1} [24]. For (*E*)-2HBA3IPA), the N—H stretching vibration is recorded at 3402 cm^{-1} as a very strong band in FT-IR spectrum and its corresponding calculated frequency is 3545 cm^{-1} using B3LYP/6-31G(d,p) (mode no: 110). This assignment is in excellent agreement with Billes et al. [4], in the case of indole. The TED corresponding to this vibration is a pure mode and it is exactly contributing to 100%. The vibrational bands due to the N—H stretching are sharper than O—H group in FT-IR spectrum. The N—H in-plane bending vibration is assigned to 1067/1067 cm^{-1} as weak band in FT-IR/FT-Raman spectra. The observed δ_{N-H} mode is coincided with the computed value 1071 cm^{-1} (mode no: 61). The out-of-plane plane bending mode (Γ_{N-H}) is attributed to 362 cm^{-1} (mode no:18). The δ_{N-H} and Γ_{N-H} vibrations are in line with observed frequency 1080 and 347 cm^{-1} in FT-IR spectrum, respectively [25]. These assignments are also find support from TED values.

O—H vibrations

The O—H stretching vibrations are extremely sensitive to hydrogen bonding. The non-hydrogen bonded (or) free hydrogen group absorbs strongly in the region 3550–3700 cm^{-1} [26]. Hydrogen atom bonded with carboxylic group displays a very broad, intense O—H stretching band in the range of 2500–3300 cm^{-1}. The weaker C—H stretching modes are generally superimposed upon the broad O—H band [27]. The free hydroxyl group absorbs strongly in the region 3700–3584 cm^{-1}, whereas the existence of intermolecular hydrogen bond formation can lower the O—H stretching frequency to the 3550–3200 cm^{-1} region with increase in intensity and breath [28,29]. In the present investigation, the stretching vibration of O—H group is assigned as a weak band 3898 cm^{-1} for carboxylic group, whereas the ν_{O-H} of phenol ring observed at 3056 cm^{-1} and 3054 cm^{-1} are belongs to FT-IR and FT-Raman spectra, respectively. The phenol ring hydroxyl group stretching is shifted to lower region as a mixture of C—H band; this is due to the intra-molecular hydrogen bonding interaction between ($N_{23}\cdots H_{22}—O_{21}$) nitrogen and hydroxyl group. And their corresponding harmonic frequencies are 3605 and 3058 cm^{-1} (mode nos: 111 and 102). These assignments show good agreement with Wang et al. [19] and also find support from TED values (100%: carboxylic and 79%: phenol).

In general, the O—H in-plane bending vibration for phenol lies in the region 1150–1250 cm^{-1} and it is not much affected due to hydrogen bonding unlike that to stretching and out-of-plane bending wavenumber [30]. In this work, the δ_{O-H} vibrations appear as weak bonds in FT-Raman/FT-IR at 1164/1165 cm^{-1} (carboxylic group) and as a strong band in FT-IR at 1414 cm^{-1} (phenol). The theoretically computed wavenumber shows good agreement with experimental observations at 1178 and 1408 cm^{-1} (mode nos: 67, 83). These assignments are within the expected range and also in consistent with literature values [19].

The O—H out-of-plane deformation for phenol lies in the region 290–320 cm^{-1} for free O—H and in the region 517–710 cm^{-1} for associated O—H [31]. In both intra and intermolecular associations, the wavenumbers are at higher value than that in the free O—H. The wavenumber increases with hydrogen bond strength because of large amount of energy required to twist the O—H bond [32]. In accordance with above conclusion the predicted band at 812 cm^{-1} (mode no: 45) and 585 cm^{-1} (mode no: 31) for (*E*)-2HBA3IPA are assigned to Γ_{O-H} mode for phenol and carboxylic group, respectively. The mode number 45 is largely deviated from literature value (517–710 cm^{-1}). This difference is due to the presence of intra-molecular hydrogen bonding.

Methylene group vibrations

The CH_2 group frequencies basically six fundamentals can be associated, namely symmetric, asymmetric, scissoring, rocking, wagging and twisting vibrations. The spectral concert of the sp^3 hybridized methylene asymmetric and symmetric stretching vibrations normally appeared in the region 3100–2900 cm^{-1} [33].

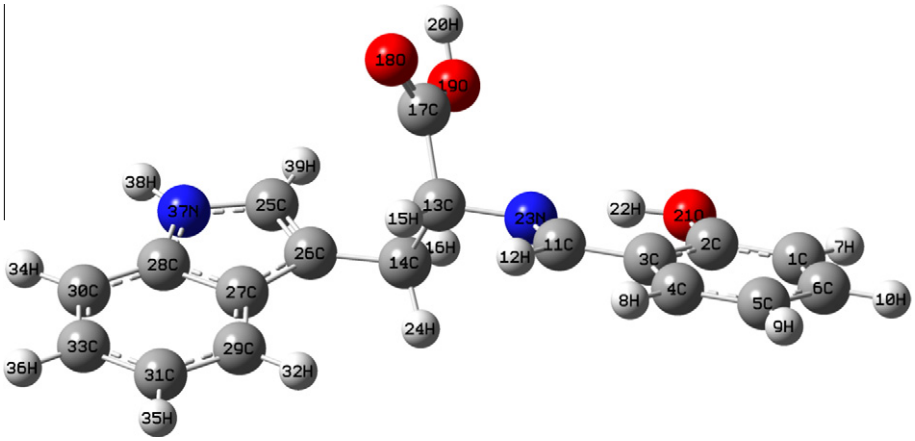

Fig. 1. The optimized structure of (E)-2-(2-hydroxybenzylideneamino)-3-(1H-indol-3yl) propanic acid [(*E*)-2HBA3IPA].

Table 1
Vibrational wave numbers obtained for (*E*)-2HBA3IPA at B3LYP/6-31G(d,p) [harmonic frequency (cm^{-1}), IR, Raman intensities (km/mol)].

	Un scaled	Scaled	FT-IR	FT-Raman	IR Rel.	Raman Rel.	Vibrational assignments TED ⩾ 10%
1	16	15			0.32	63.30	$\Gamma_{C11-N23-C13-C14\Gamma(23)} + \Gamma_{C11-N23-C13-H15(13)} + \Gamma_{C11-N23-C13-C17(16)}$
2	19	18			0.08	88.32	$\Gamma_{H16-C14-C13-N23(10)} + \Gamma_{C26-C14-C13-C17(11)} + \Gamma_{C26-C14-C13-N23(22)}$
3	33	32			0.03	56.18	$\Gamma_{C13-N23-C11-C3(21)}$
4	36	34			0.08	49.13	$\Gamma_{C11-N23-C13-C17(16)} + \Gamma_{C25-C26-C14-C13(14)} + \Gamma_{C27-C26-C14-C13(20)} + \Gamma_{C27-C26-C14-H16(11)}$
5	51	49			0.21	18.38	$\Gamma_{O18-C17-C13-C14(21)} + \Gamma_{O19-C17-C13-C14(16)} + \Gamma_{O18-C17-C13-N23(16)} + \Gamma_{O19-C17-C13-N23(11)}$
6	70	67			0.01	31.01	$\Gamma_{C13-N23-C11-C3(10)}$
7	93	89			0.09	5.27	$\delta_{N23-C11-C3(17)} + \delta_{C11-N23-C13(18)}$
8	119	115		102vs	0.01	26.25	$\Gamma_{N23-C11-C3-C4(16)} + \Gamma_{C11-N23-C13-C17(10)}$
9	142	136		125w	0.15	7.41	$\delta_{C14-C13-C17(15)}$
10	185	178		157w	0.17	7.05	$\nu_{C-C(13)} + \delta_{CCC(12)} + \Gamma_{CCCC(11)}$
11	216	208			0.29	2.66	$\Gamma_{C4-C3-C2-O21(14)} + \Gamma_{O21-C2-C1-C6(13)}$
12	222	213			0.74	2.91	$\delta_{C4-C3-C11(11)}$
13	227	218			1.61	0.61	$\Gamma_{C29-C27-C26-C25(12)} + \Gamma_{C33-C30-C28-N37(15)}$
14	287	275			0.45	0.36	$\delta_{O19-C17-C13(15)}$
15	302	290			1.57	2.60	$\nu_{CC(10)} + \Gamma_{CCCN(14)}$
16	331	318			0.48	4.77	$\Gamma_{N23-C11-C3-C2(17)}$
17	354	340			0.06	6.23	$\Gamma_{C13-N23-C11-C3(13)}$
18	377	362			8.61	2.41	$\Gamma_{H38-N37-C28-C27(14)} + \Gamma_{H38-N37-C28-C30(17)} + \Gamma_{H38-N37-C25-H39(11)}$
19	409	393			4.36	2.21	$\delta_{C11-C3-C2(10)}$
20	437	419			0.01	0.54	$\Gamma_{C33-C30-C28-C27(11)} + \Gamma_{C31-C33-C30-C28(11)}$
21	437	420	426m		3.61	0.76	$\nu_{CC(10)} + \delta_{CCC(27)}$
22	467	449			0.78	0.83	$\delta_{C14-C26-C25(12)} + \delta_{C27-C26-C14(10)} + \delta_{C29-C27-C26(10)} + \delta_{C30-C28-N37(19)}$
23	469	451			1.65	1.02	$\delta_{O21-C2-C1(21)} + \delta_{C3-C2-O21(17)}$
24	476	457	463w		0.10	2.73	$\delta_{O21-C2-C1(10)}$
25	523	502	504ms		3.11	2.85	$\nu_{C17-C13(12)} + \delta_{O18-C17-C13(18)}$
26	553	531	528s		0.18	2.31	$\nu_{CC(26)} + \delta_{CCC(29)}$
27	559	537			0.23	0.84	$\Gamma_{C1-C6-C5-C4(15)}$
28	572	549	547m	548w	0.53	5.87	$\delta_{C3-C2-C1(10)}$
29	589	565			1.51	0.37	$\Gamma_{C30-C33-C31-C29(17)}$
30	601	577			1.78	1.52	$\nu_{CC(10)} + \delta_{CCC(19)}$
31	609	585	582m		18.2	2.20	$\Gamma_{H20-O19-C17-C13(31)} + \Gamma_{H20-O19-C17-O18(12)}$
32	630	605	597w	597w	9.95	2.44	$\delta_{O19-C17-C13(11)} + \delta_{O18-C17-O19(18)} + \Gamma_{H20-O19-C17-C13(13)} + \Gamma_{H20-O19-C17-O18(12)}$
33	643	618	625w		0.37	1.04	$\Gamma_{CCCN(18)}$
34	674	647	660w		1.54	1.38	$\Gamma_{H20-O19-C17-O18(10)}$
35	738	709			0.43	0.47	$\Gamma_{CCCC(42)+CCCH(21)}$
36	753	724			0.78	1.70	$\nu_{C26-C14(12)}$
37	755	725			10.9	0.93	$\Gamma_{H35-C31-C29-C27(15)} + \Gamma_{C30-C33-C31-H35(11)} + \Gamma_{H36-C33-C30-C28(17)} + \Gamma_{H36-C33-C31-C29(11)} + \Gamma_{H34-C30-C28-N37(11)}$
38	769	739	739s		12.6	0.91	$\Gamma_{H9-C5-C4-C3(20)} + \Gamma_{C1-C6-C5-H9(17)} + \Gamma_{H10-C6-C1-C2(11)}$
39	771	741	745s	743w	1.35	6.58	$\nu_{C27-C26(11)} + \nu_{C28-C27(10)}$
40	779	748			2.68	1.00	$CCCC(23)+CCCH(13)$
41	786	755		756m	1.72	0.59	$\nu_{C3-C2(12)}$
42	796	765	766w		4.49	0.52	$\Gamma_{C14-C26-C25-H39(11)} + \Gamma_{C27-C26-C25-H39(11)}$
43	812	780	777w	781w	2.47	6.87	$\Gamma_{C14-C26-C25-H39(15)}$
44	835	802			1.80	12.77	$\nu_{C17-C13(18)} + \nu_{O19-C17(11)}$
45	846	812			15.1	0.61	$\Gamma_{H22-O21-C2-C1(42)} + \Gamma_{H22-O21-C2-C3(48)}$
46	859	826			0.05	1.28	$\Gamma_{H32-C29-C27-C26(12)} + \Gamma_{H36-C33-C31-H35(12)} + \Gamma_{H34-C30-C28-N37(15)}$
47	873	838	836w	837w	0.11	1.62	$\Gamma_{C5-C6-C1-H7(13)} + \Gamma_{H10-C6-C5-H9(11)} + \Gamma_{O21-C2-C1-H7(20)}$
48	888	853	846w		0.15	0.87	$\delta_{C33-C31-C29(12)} + \delta_{C25-N37-C28(11)}$
49	907	872	864m	867m	2.55	0.33	$\delta_{C1-C6-C5(13)} + \delta_{C6-C5-C4(12)}$
50	928	891	876w		0.19	0.22	$\Gamma_{H35-C31-C29-H32(19)} + {}_{H36-C33-C30-H34(24)}$
51	945	908	903vw		0.10	0.61	$\Gamma_{H9-C5-C4-H8(32)}$
52	969	931			2.07	0.84	$\Gamma_{H36-C33-C31-H35(11)}$
53	971	933			1.38	0.41	$\Gamma_{H35-C31-C29-H32(15)} + \Gamma_{H36-C33-C31-H35(16)}$
54	986	947			0.05	0.02	$\Gamma_{H10-C6-C1-H7(30)} + \Gamma_{H10-C6-C5-H9(28)}$
55	1007	967	963w		1.27	5.84	$\Gamma_{H12-C11-C3-C2(12)} + \Gamma_{H12-C11-C3-C4(19)} + \Gamma_{C13-N23-C11-H12(26)}$
56	1041	1000	989w	985w	0.80	5.24	$\nu_{C31-C29(12)} + \nu_{C33-C30(12)} + \nu_{C33-C31(40)}$
57	1050	1009	1007m	1009s	3.16	23.85	$\nu_{C14-C13(35)}$
58	1057	1015			0.06	3.17	$\nu_{C6-C5(31)}$
59	1074	1032			3.70	2.99	$\nu_{N23-C13(30)}$
60	1093	1050	1055w		6.74	1.97	$\nu_{N23-C13(25)}$
61	1114	1071	1067w	1067	6.73	0.06	$\nu_{N37-C25(26)} + \delta_{H38-N37-C25(12)} + \delta_{C26-C25-H39(12)} + \delta_{N37-C25-H39(18)}$
62	1145	1100			2.02	1.73	$\nu_{C5-C4(17)}$
63	1150	1105	1096m		6.88	1.22	$\nu_{C31-C29(10)}$
64	1165	1120	1122w	1120w	9.32	6.35	$\nu_{O19-C17(11)} + \delta_{H20-O19-C17(12)}$
65	1183	1136	1135m		4.09	2.64	$\delta_{H9-C5-C4(14)} + \delta_{C6-C5-H9(13)} + \delta_{H10-C6-C1(12)} + \delta_{H10-C6-C5(12)}$
66	1184	1137			3.80	0.27	$\delta_{H35-C31-C29(16)} + \delta_{C33-C31-H35(14)}$
67	1226	1178	1165w	1164w	16.7	5.30	$\delta_{H20-O19-C17(21)}$
68	1241	1193			7.79	4.73	$\nu_{C2-C1(22)} + \nu_{C11-C3(22)}$
69	1253	1204	1210w	1209w	5.01	0.68	$\nu_{N37-C25(11)} + \nu_{N37-C28(17)}$
70	1270	1220			1.60	19.45	$\nu_{C4-C3(19)} + \delta_{H8-C4-C3(17)} + \delta_{C5-C4-H8(14)}$
71	1279	1229	1231w	1233w	2.28	1.46	$\delta_{H32-C29-C27(11)} + \delta_{H34-C30-C28(11)}$
72	1309	1258	1250w	1253w	1.15	2.85	$\delta_{CCH(21)}$
73	1333	1280			0.16	2.58	$\nu_{N37-C25(13)}$
74	1339	1286			11.3	0.97	$\nu_{O21-C2(37)}$
75	1345	1292		1295w	1.96	2.21	$\delta_{H15-C13-C17(17)} + \Gamma_{C11-N23-C13-H15(14)}$
76	1365	1311			4.90	8.01	$\delta_{CCH(15)} + \Gamma_{OCCH(10)}$
77	1372	1319	1315 s	1313ms	1.52	26.26	$\nu_{C3-C2(16)} + \nu_{C5-C4(13)} + \nu_{C6-C1(14)}$

Table 1 (*continued*)

	Un scaled	Scaled	FT-IR	FT-Raman	IR Rel.	Raman Rel.	Vibrational assignments TED ⩾ 10%
78	1381	1326			5.84	1.66	$\nu_{O19-C17(11)} + \delta_{H20-O19-C17(14)}$
79	1385	1331			6.04	0.68	$\nu_{CC(45)} + \delta_{CCH(16)}$
80	1393	1338	1341s	1342w	0.22	5.24	$\nu_{CC(42)} + \delta_{CCH(12)}$
81	1424	1368	1358ms	1359s	2.54	6.69	$\delta_{H12-C11-C3(14)} + \delta_{H12-C11-N23(28)}$
82	1460	1403			4.00	8.01	$\nu_{C27-C26(11)} + \nu_{N37-C25(12)} + \delta_{H38-N37-C25(15)} + \delta_{H38-N37-C28(14)}$
83	1465	1408	1414 vs		9.09	6.40	$\nu_{C6-C1(11)} + \delta_{H22-O21-C2(36)}$
84	1494	1435		1428s	1.75	1.74	$\delta_{H16-C14-H24(14)}$
85	1497	1439			3.98	2.48	$\delta_{H16-C14-H24(17)}$
86	1511	1451	1455s	1455m	11.96	34.77	$\nu_{C3-C2(14)} + \nu_{C5-C4(12)} + \nu_{O21-C2(14)}$
87	1536	1476			0.78	0.34	$\nu_{C31-C29(13)} + \delta_{C33-C31-H35(14)}$
88	1546	1485	1487ms	1488w	9.33	1.42	$\nu_{C6-C5(15)} + \delta_{H9-C5-C4(11)} + \delta_{H22-O21-C2(23)}$
89	1603	1540			3.21	15.95	$\nu_{C26-C25(39)} + \text{C30-C28(10)}$
90	1631	1567	1554m	1556s	0.14	2.02	$\nu_{C28-C27(11)} + \nu_{C29-C27(16)} + \nu_{C33-C30(14)} + \nu_{C33-C31(14)}$
91	1631	1568	1583vs	1573w	17.35	22.18	$\nu_{C3-C2(11)} + \nu_{C6-C1(18)} + \nu_{C6-C5(13)} + \delta_{H22-O21-C2(19)}$
92	1677	1611			1.20	1.73	$\nu_{C30-C28(22)} + \nu_{C31-C29(15)}$
93	1679	1613			14.66	12.37	$\nu_{C2-C1(20)} + \nu_{C5-C4(20)} + \delta_{H22-O21-C2(11)}$
94	1695	1629	1611m	1617vs	67.12	100.0	$\nu_{C11-N23(63)}$
95	1853	1780	1664vs		48.90	0.93	$\nu_{C17=O18\ (86)}$
96	3036	2917	2906w	2906	4.58	0.54	$\nu_{C11-H12\ (88)} + \nu_{C13-H15\ (12)}$
97	3037	2918			11.61	2.17	$\nu_{C11-H12\ (12)} + \text{C13-H15 (87)}$
98	3053	2933	2963w	2938w	3.92	1.80	$\nu_{C14-H16\ (17)} + \nu_{C14-H24\ (83)}$
99	3114	2992		2969w	2.16	0.97	$\nu_{C14-H16\ (82)} + \nu_{C14-H24\ (17)}$
100	3174	3049			5.06	1.52	$\nu_{C4-H8\ (83)}$
101	3177	3052			1.90	0.80	$\nu_{C29-H32\ (44)} + \nu_{C30-H34\ (10)} + \nu_{C31-H35\ (30)} + \nu_{C33-H36\ (15)}$
102	3182	3058	3054s	3056s	100.00	4.88	$\nu_{O21-H22\ (79)}$
103	3183	3058			2.31	2.61	$\nu_{C29-H32\ (27)} + \nu_{C30-H34\ (49)} + \nu_{C33-H36\ (20)}$
104	3188	3063			5.29	1.54	$\nu_{C6-H10\ (73)} + \nu_{O21-H22\ (11)}$
105	3194	3068			6.34	1.76	$\nu_{C29-H32\ (21)} + \nu_{C30-H34\ (28)} + \nu_{C31-H35\ (32)} + \nu_{C33-H36\ (18)}$
106	3206	3080			4.53	7.64	$\nu_{C30-H34\ (11)} + \nu_{C31-H35\ (37)} + \nu_{C33-H36\ (45)}$
107	3210	3084			3.47	3.43	$\nu_{C1-H7\ (25)} + \nu_{C5-H9\ (68)}$
108	3217	3091			3.22	6.91	$\nu_{C1-H7\ (67)} + \nu_{C5-H9\ (16)} + \nu_{C6\ -H10\ (15)}$
109	3265	3137			0.11	2.02	$\nu_{C25-H39\ (99)}$
110	3690	3545	3402vs		15.46	2.79	$\nu_{N37-H38\ (100)}$
111	3752	3605	3898w		11.96	2.16	$\nu_{O19-H20\ (100)}$

ν – stretching, δ – in-plane bending, Γ – out-of-plane bending, s – strong, m – medium, w – weak, v – very.
a. Obtained from the wave numbers calculated at B3LYP/6-31g(d,p) using scaling factor 0.9608 [21].
b. Relative absorption intensities normalized with highest peak absorption equal to 100.
c. Relative Raman intensities normalized to 100.
d. Total energy distribution calculated B3LYP 6-31g(d,p) level, TED less than 10% are not shown.

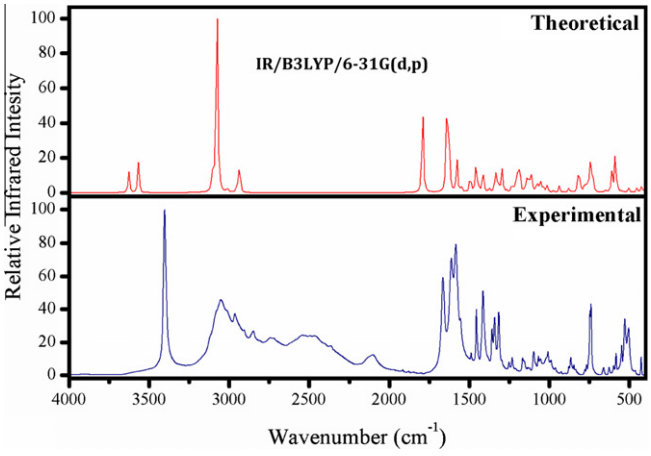

Fig. 2. The combined theoretical and experimental FT-IR spectrum of (*E*)-2HBA3IPA.

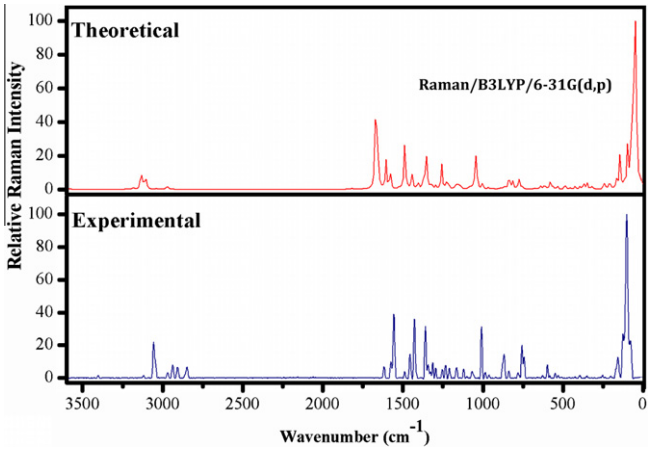

Fig. 3. The combined theoretical and experimental FT-Raman spectrum of (*E*)-2HBA3IPA.

The asymmetric and symmetric stretching vibrations are observed as a weak band. The bands at 2963 and 2969 cm^{-1} are assigned to CH_2 asymmetric stretching in FT-IR spectrum, which are moderately match with the calculated value at 2992 cm^{-1} (mode no: 99). The theoretically predicted value (mode no: 98) at 2933 cm^{-1} is attributed to CH_2 symmetric stretching, which also goes well with the experimental value at 2938 cm^{-1} in FT-Raman spectrum. The TED corresponding to the CH_2 scissoring vibration appeared ~83%. The fundamental CH_2 vibrations such as scissoring, wagging, twisting and rocking are able to appear in the expected frequency regions 1500–800 cm^{-1} [34].

For p-bromophenoxyacitic acid, the CH_2 scissoring mode has been assigned to the weak intensity FT-IR band at about 1452 cm^{-1} [35]. The scissoring mode of CH_2 group gives rise to a characteristic band near 1428 cm^{-1} in FT-Raman, while the harmonic value is 1435 cm^{-1} (mode no: 84). The wagging vibrational band of CH_2 mode is recorded at 1250 and 1253 cm^{-1} as a weak band in FT-IR and FT-Raman, respectively, the mode number 72

(1258 cm^{-1}) is its corresponding harmonic wavenumber for ωCH_2 vibration. Twisting band at 1165, 1122, 1096 cm^{-1} are observed by FT-IR, whereas, the 1164 and 1120 cm^{-1} are observed by FT-Raman. These twisting frequencies are comparable with computed values of 1178, 1120 and 1105 cm^{-1} using B3LYP/6-31G(d,p) (mode nos: ν_{67}, ν_{64} and ν_{63}). These assignments have considerable TED values.

C—H vibrations

The hetero aromatic structure shows the presence of C—H stretching vibrations in the range 3000–3100 cm^{-1}, which is the characteristic region for ν_{C-H} stretching [36]. There are five C—H stretching modes in indole, four from benzene ring and one from pyrrole ring. The absorption in the range 3000–3125 cm^{-1} has been identified with that of C—H indole motif of 5-aminoindole [37]. The vibrations assigned to indole C—H stretch in (*E*)-2HBA3IPA by B3LYP in the region 3052–3137 (mode nos: 101, 103, 105, 106, 109) are in agreement with vapor bands of indole at 3140, 3119, 3090, 3072, 3061 and 3051 cm^{-1} [38,39], this assignment also in line with Sundaraganesan et al. [40]. The expected four C—H stretching modes for phenol are C_4—H_8, C_5—H_9, C_6—H_{10} and C_1—H_7 units. The mode numbers 100, 104, 107, 108 are assigned to aromatic C—H stretch in the region 3049–3091 cm^{-1} are in agreement with harmonic frequencies (B3LYP/6-311G(d,p)) at 3046–3098 cm^{-1} [19]. The mode number 96, 97 are assigned to C_{11}—H_{12} and C_{13}—H_{15} stretching vibrations shows moderate agreement with experimental values (FT-IR: 2906/FT-Raman 2906 cm^{-1}).

In aromatic compounds, the C—H in-plane bending vibrations appeared in the range 1000–1300 cm^{-1} and out-of-plane bending vibrations appeared in the range 750–1000 cm^{-1} [41,42]. The C—H in-plane bending vibrations of 5-amino indole occur in the region (harmonic) 1047–1218 cm^{-1} [40]. In this study, the harmonic frequencies of indole assigned in the range 1071–1338 cm^{-1} (mode nos: 61, 66, 71, 76, 80), despite the fact that this is contaminated by C—N and C—C stretching vibrations. These assignments are supported by observed FT-IR (1067, 1231 cm^{-1}) and FT-Raman bands (1067, 1233 cm^{-1}). For (*E*)-2HBA3IPA, the observed bands 1135 (FT-IR), 1250/1253 cm^{-1} (FT-IR/FT-Raman), which are closer to calculated δ_{C-H} wavenumbers (mode nos: 65, 70, 72, 79) lie in the range of 1136–1331 cm^{-1}. These assignments show good agreement with Wang et al. [19]. The observed bands 1295 (FT-Raman) and 1358/1359 cm^{-1} (FT-IR/FT-Raman) and their corresponding calculated bands 1292 and 1368 cm^{-1} (mode nos: 75, 81) are assigned to $\delta_{C13-H15}$ and $\delta_{C11-H12}$ modes, respectively.

The C—H out-of-plane bending vibrations of indole occurring at 765–933 cm^{-1} (mode nos: 42, 43, 46, 50, 53) are in line with the reported range 694–885 cm^{-1} (harmonic) by Sundaraganesan et al. [40]. The theoretically predicted values in the range 739–947 cm^{-1} (mode nos: 38, 47, 51, 54) are attributed to C—H out-of-plane bending vibrations of phenol in (*E*)-2HBA3IPA, which also goes well with the literature values in the range 738–943 cm^{-1} [19]. These assignments find supported from observed values 739, 766, 777, 836, 876, 963 cm^{-1} in FT-IR and 781, 837 cm^{-1} in FT-Raman spectra. The band 967 (harmonic)/ (FT-IR: 963 cm^{-1}) is attributed to C_{11}—H_{12} out-of-plane bending mode. These assignments are also supported by TED values.

C=O and C—O vibrations

The carbon–oxygen double bond formed by pπ–pπ between carbon and oxygen, and the lone pair of electron on oxygen also determines the nature of carbonyl group. The C=O stretching is a characteristic frequency of carboxylic acid [43]. The carbonyl C=O stretching vibration is expected to occur in the region 1680–1715 cm^{-1} [44,45], and in the present study this mode appears as strong band at 1064 cm^{-1} in FT-IR spectrum. According to TED results, the $\nu_{C=O}$ is pure mode contributing 86%. The theoretically computed value of 1780 cm^{-1} (mode no: 95) shows positive deviations of ~116 cm^{-1}. This deviation can be attributed to the under estimation of the large degree of π-electron delocalization due to conjugation of the molecule [46]. The intensity of the carbonyl group can increase because of conjugation or formation of hydrogen bonds. The present assignment agrees well with the value available in the literature [35].

The C—O stretching mode of phenol moiety is identified as strong band at 1455 in FT-IR and medium band at 1455 cm^{-1} in FT-Raman spectra. The calculated value at 1451 cm^{-1} (mode no: 86) shows good agreement with experimental value and also in consistent with literature [19]. The FT-IR band near 1122 cm^{-1} is due to the mode of $\nu_{C17-C19}$ (carboxylic acid). The theoretically computed value at 1120 cm^{-1} (mode no: 64) shows excellent agreement with FT-Raman band at 1120 cm^{-1}. In p-bromophenoxyacetic acid this vibration was found at 1122 cm^{-1}/B3LYP/6-31G(d,p) level of theory [35]. The harmonic bands identified at 605/585 cm^{-1} (mode nos: 32/31) and 457/208 cm^{-1} (mode nos: 24/11) are assigned to $\delta_{C17-O19}/\Gamma_{C17-O19}$ modes for carboxylic acid and phenol, respectively. Sundaraganesan et al. [35] and Wang et al. [19] reported the $\delta_{C-O}/\Gamma_{C-O}$ modes are at 573/505 cm^{-1} (harmonic) and 453 (FT-IR)/ 212 cm^{-1} (FT-Raman), respectively. These assignment also find support from observed FT-IR (597, 582 and 463 cm^{-1}) bands. The δ_{C-O} mode (carboxylic acid) mixed with $\delta_{(O18=C17-O19)}$ mode. Further, $\delta_{(O18=C17-O19)}$ vibration is identified at 597/597 cm^{-1} (FT-IR/FT-Raman) in (*E*)-2HBA3IPA. Their nature could be seen from Table 1. The predicted harmonic values 502 (FT-IR: 504), 275 and 49 cm^{-1} (mode nos: 25, 14, 5) are attributed to $\delta_{O18=C17-C13}$, $\delta_{O19-C17-C13}$ and $\Gamma_{O18=C17-C13}/\Gamma_{O19-C17-C13}$ (carboxylic) respectively. In our title molecule, the scaled vibrational frequencies computed by B3LYP method at 457 (463: FT-IR) and 208 cm^{-1} (mode nos: 24, 11) are assigned to in-plane and out-of-plane bending vibrations of O21—C2—C1 unit respectively.

C=N, C—N vibrations

Due to the intra-molecular interaction between nitrogen and oxygen in Schiff bases, the C=N stretching is shifted to 1611 cm^{-1} using FT-IR [17]. The strong band at 1605 cm^{-1} in FT-IR spectrum is assigned to C=N stretching vibration [18]. The transfer of electron from nitrogen to oxygen atom is accompanied by a rearrangement of the whole six-membered ring and substantial changes were observed in the carbon–oxygen and carbon–nitrogen bonds. In the present investigation, the C=N and O—H are involved in the intra-molecular interaction. Wang et al. [19] has proposed an assignment for C=N mode at 1625 cm^{-1} in FT-Raman spectrum, which matches the calculated value at 1629 cm^{-1} (mode no: 94) in this study. For the same mode, the experimental values are 1611/FT-IR and 1617 cm^{-1}/FT-Raman. These observed and theoretical wavenumbers are well coincided with literature and also find support from TED (63%) value. It is evident from Table 1, that the C_{13}—N_{23} vibration due to stretching is observed at lower frequency side (1055: FT-IR) than the $\nu_{C11-N23}$ (1611 cm^{-1}/ FT-IR), which may be due to the presence of intra-molecular hydrogen bond interaction between O_{21}—H_{22} and N_{23}. The calculated C_{13}—N_{23} stretching mode of 1050 cm^{-1} (mode no: 60) coupled with the δ_{C-H} moiety are well with in the reported range 1230–1030 cm^{-1} [47] and also in satisfactory agreement with the experimental (FT-IR/1055 cm^{-1}) spectrum.

In 3-methylindole, the C—N stretching bands are found to be present at 1229 and 1080 cm^{-1} [25]. The observed bands at 1210/1209 (FT-IR/FT-Raman) and 1067/1067 cm^{-1} (FT-IR/FT-Raman), respectively, corresponds to $\nu_{C28-N37}$ and $\nu_{C25-N37}$ units and their corresponding calculated values are 1204 and 1071 cm^{-1} (mode nos: 69, 61). These assignments are also having considerable TED values. The in-plane C_{25}—N_{37}—C_{28} (Indole) and

out-of-plane C_{13}—N_{23}—C_{11} bending vibrations are attributable 853 (846/FT-IR), 340 cm^{-1} (mode nos: 48, 17), respectively.

C—C vibrations

In substituted benzenes the degenerate C—C stretching and non-degenerate skelekel vibrations lie in the region 1365–1620 cm^{-1} and 1205–1280 cm^{-1}, respectively [48]. But in phenols, these vibrations are relatively at higher wavenumber due to its coupling with the in-plane OH bending mode [48]. Similar trend also observed in the present case. The stretching vibrations due to C—C bonds are computed at 1319–1613 cm^{-1} (mode nos: 77, 83, 86, 88, 91, 93) show good coherence with recorded FT-IR/FT-Raman spectra at 1315–1487/1313–1573 cm^{-1}. These assignments are line with literature values [48] and also find support from Wang et al. [19].

Sundaraganesan et al. [40] was observed ν_{C-C} vibrations at 1276–1616 cm^{-1} in indole. Bunte et al. [25] observed this band at 1345–1617 cm^{-1} for 3-methyl indole. Based on the these factors, in the present study, the calculated wavenumbers 1611, 1567, 1476, 1338, 1331 and 1540, 1403 cm^{-1} (mode nos: 92, 90, 87, 80 and 89, 82) are assigned to ν_{C-C} stretching mode in benzene and indole ring respectively. And their corresponding FT-IR bands are 1583, 1554 (1556/FT-Raman), 1341 cm^{-1} (FT-Raman: 1342). The wave numbers 57 and 68 are belonging to $\nu_{C14-C13}$ and ν_{C11-C3}, in which wavenumber 57 is supported 1007/1009 cm^{-1} (FT-IR/FT-Raman) by experimental observations. The TED corresponding to all C—C vibrations lies between 10% and 45%, as shown in Table 1.

Literature survey reveals that the C—C—C deformation vibrations assigned at 542, 607, 848 cm^{-1} in indole [40]. The observed bands of 864, 547 cm^{-1} in FT-IR and 846, 528, 426 cm^{-1} in FT-Raman are assigned to δ_{C-C-C} vibrations of the phenyl ring and indole ring, respectively. And the FT-Raman bands 867, 548 cm^{-1} are due to the δ_{C-C-C} in phenol. For the same mode, the calculated wavenumbers (mode nos: 49, 30, 28 and 48, 26, 21) show good consistent with recorded spectral data. In indole the bands observed at 758, 487, 423 cm^{-1} are assigned to C—C—C out-of-plane vibrations [40]. In 6-chloroindole, the Γ_{C-C-C} band is found to be present at 598 cm^{-1} [49] and Subramanian et al. [48] have calculated this band at 592, 670 cm^{-1} in the case of 2,4-difluorophenol. Considering these factors, in this study, the computed bands at 748, 565, 419 cm^{-1} and 709, 537 cm^{-1} are assigned to Γ_{C-C-C} vibrations respectively in indole and phenol ring of (*E*)-2HBA3IPA. The wavenumbers 449, 213, 136, 178 (157/FT-Raman) and 34, 115 (102/FT-Raman), 18, 32 cm^{-1} (mode nos: 22, 12, 9, 10 and 4, 8, 2, 3) are assigned to in-plane and out-of-plane bending vibrations of C_{14}—C_{26}—C_{25}, C_{11}—C_3—C_4, C_{14}—C_{13}—C_{17}, C_{26}—C_{14}—C_{13} units respectively. The TED of these vibrations are not pure modes as it is evident from the frequency calculation. In addition to these bending vibrations, C—C—H, C—C—N, C—C—O and C—N—H bending vibrations have been assigned in the characteristic range in analogy with related molecules for (*E*)-2HBA3IPA.

Hyperpolarizability

The first hyperpolarizabilities (β_0, α and μ) of (*E*)-2HBA3IPA is calculated using B3LYP/6-31G(d,p) level of theory, based on the finite-field approach. In the presence of an applied electric field, the energy of a system is a function of the electric field. First hyperpolarizability is a third rank tensor that can be described by a $3 \times 3 \times 3$ matrix. The 27 components of the 3D matrix can be reduced to 10 components due to Kleinman symmetry [50]. It can be given in the lower tetrahedral format. It is obvious that the lower part of the $3 \times 3 \times 3$ matrixes is a tetrahedral. The components of β are defined as the coefficients in the Taylor series expansion of the energy in the external electric field. When the external electric field is weak and homogeneous, this expansion becomes:

$$E = E^0 - \mu_\alpha F_\alpha - \frac{1}{2}\alpha_{\alpha\beta}F_\alpha F_\beta - \frac{1}{6}\beta_{\alpha\beta\gamma}F_\alpha F_\beta F_\gamma \quad (2)$$

where E^0 is the energy of the unperturbed molecules, F_α is the field at the origin, and μ_α, $\alpha_{\alpha\beta}$, $\beta_{\alpha\beta\gamma}$ are the components of the dipole moment, polarizability and the first hyperpolarizabilities, respectively. The total static dipole moment μ, the mean polarizability α_0, the anisotropy of polarizability $\Delta\alpha$ and the mean first hyperpolarizability β_0, using the *x*, *y*, *z* components are defined as

$$\mu = (\mu_x^2 + \mu_y^2 + \mu_z^2)^{1/2} \quad (3)$$

$$\alpha_0 = \frac{\alpha_{xx} + \alpha_{yy} + \alpha_{zz}}{3} \quad (4)$$

$$\Delta\alpha = 2^{-1/2}[(\alpha_{xx} - \alpha_{yy})^2 + (\alpha_{yy} - \alpha_{zz})^2 + (\alpha_{zz} - \alpha_{xx})^2 + 6(\alpha_{xy}^2 + \alpha_{yz}^2 + \alpha_{xz}^2)]^{1/2} \quad (5)$$

$$\beta_0 = (\beta_x^2 + \beta_y^2 + \beta_z^2)^{1/2} \quad (6)$$

Many organic molecules, containing conjugated π electrons are characterized by large values of molecular first hyper polarizabilities, were analyzed by means of vibrational spectroscopy [51–54]. The intra-molecular charge transfer from the donor to acceptor group through a single-double bond conjugated path can induce large variations of both the molecular dipole moment and the molecular polarizability, making IR and Raman activity strong at the same time [55].

The present study reveals that the π–π interaction can make larger intra-molecular interaction and hence the polarizability of the molecule increases. It is evident from Table 2 the molecular dipole moment (μ), molecular polarizability and hyperpolarizability are calculated about 0.7815 (*D*), 4.384 and 3.173×10^{-3} esu, respectively. The β_0 value of the title compound is ~8.5 times greater than that of urea.

NBO analysis

The hyperconjugation may be given as stabilizing effect that arises from an overlap between an occupied orbital with another neighboring electron deficient orbital, when these orbitals are properly orientated. This non-covalent bonding–antibonding interaction can be quantitatively described in terms of the NBO analysis, which is expressed by means of the second-order perturbation interaction energy ($E^{(2)}$) [56–59]. This energy represents the estimate of the off-diagonal NBO Fock matrix elements. It can be deduced from the second-order perturbation approach [60]

$$E^{(2)} = \Delta E_{ij} = q_i \frac{F(i,j)^2}{\varepsilon_j - \varepsilon_i} \quad (7)$$

where q_i is the donor orbital occupancy, ε_i and ε_j are diagonal elements (orbital energies) and $F(i,j)$ is the off diagonal NBO Fock matrix elements. NBO analysis of (*E*)-2HBA3IPA has been performed, in order to explain the intra-molecular charge transfer and delocalization of π-electrons from amino group to salicylidine ring. The NBO calculation was performed for two different conformers namely enol–imine close form and enol–imine open form. From the NBO calculations, there are certain energy deviation have obtained between closed and open form of enol–amine. The intra-molecular hyperconjugative interactions is due to the overlap between π(C—C) and π*(C—C) orbitals, which results intra-molecular charge transfer appeared in the molecular system [55]. It is evident from our calculation, the $E^{(2)}$ energy of πC_3—C_4 versus $\pi^* C_5$—C_6 is about

Table 2
The molecular electric dipole moment μ (Debye), polarizability (α) and hyperpolarizability (β_0) values of (*E*)-2HBA3IPA.

Parameters	B3LYP/6-31G(d,p)
	Dipole moment
μ_x	−0.3277
μ_y	−0.1132
μ_z	0.7003
μ	0.7815
	Polarizability
α_{xx}	221.36
α_{xy}	−35.54
α_{yy}	110.87
α_{xz}	−10.5
α_{yz}	6.80
α_{zz}	318.60
α	4.384×10^{-30} esu
	Hyper polarizability
β_{xxx}	177.78
β_{xxy}	−28.26
β_{xyy}	−2.74
β_{yyy}	−4.48
β_{xxz}	−19.21
β_{xyz}	−44.84
β_{yyz}	−31.90
β_{xzz}	153.85
β_{yzz}	125.57
β_{zzz}	−83.42
β_0	3.173×10^{-30} esu

Table 3
The electronic transition of (*E*)-2HBA3IPA.

Calculated at B3LYP/6-311++G(d,p)	Oscillator strength	Experimental band gap (nm)	Calculated band gap (eV/nm)
Excited state 1	Singlet-A/f = 0.0392	330	3.5785/346.47
81 → 82 (HOMO–LUMO)	0.70201		−3.959
Excited state 2	Singlet-A/f = 0.1298	305	3.9388/314.78
78 → 82 ($HOMO_{-3}$–LUMO)	0.10338		−5.093
78 → 85 ($HOMO_{-3}$–$LUMO_{+3}$)	−0.12208		−6.045
80 → 82 ($HOMO_{-1}$–LUMO)	0.64744		−4.631
Excited state 3	Singlet-A/f = 0.0012	273	4.1483/298.88
79 → 82 ($HOMO_{-2}$–LUMO)	0.70497		−4.752

69.16 kJ/mol, and their electron densities are 1.645 and 0.379 e respectively. Similarly, the π–π^* interaction of C_5—C_6 → C_3—C_4, C_{11}—N_{23} → C_3—C_4, C_{25}—C_{26} → C_{27}—C_{29}, C_{27}—C_{29} → C_{25}—C_{26}, C_{28}—C_{30} → C_{27}—C_{29} and C_{31}—C_{33} → C_{27}—C_{29} bonds are having smaller electron densities than σ bonds. The above interactions are observed as an increase in electron density (ED) in C—C anti bonding orbital that weakens the respective donor bonds. The movement of π electron from donor (*i*) to acceptor (*j*) can make the molecule highly active. The intra-molecular hydrogen bonding interaction formed between nitrogen and hydroxyl hydrogen, which is due to the lone pair of nitrogen atom. The nitrogen accept the proton by loosing electron, where the $E^{(2)}$ energy stabilization is around 101.84 kJ/mol between N_{23} and O_{21}—H_{22}. Instead of the intra-molecular hydrogen bonding interaction between nitrogen and hydroxyl group the nitrogen can make stabilization with adjacent bond orbitals. The calculated NBOs of closed and open form enol–imine have listed is Tables S3 (a) and S3 (b) (Supplementary).

HOMO–LUMO analysis

In the present study, the band gap energy of the one electron excitation from HOMO to LUMO is calculated about −3.959 eV. The HOMO (81) is located over the tryptophane ring and LUMO (82) is located over the salicylidine ring, whereas the energy of HOMO and LUMO is about −5.137 and −1.178 eV respectively. The recorded UV spectrum shows three excited states namely E_1, E_2 and E_3. The E_1 lies between 81 and 82 orbital (HOMO–LUMO), and its recorded and calculated band gaps are about 330 and 346.47 nm, respectively. The excited state two (E_2) comprise 78–82 ($HOMO_{-3}$–LUMO), 78–85 ($HOMO_{-3}$–$LUMO_{+3}$) and 80–82 ($HOMO_{-1}$–LUMO) orbital, its recorded band gap is about 305 nm, which is coincided well with the theoretical value of 314.78 nm. Third excited state lies between 79 and 82 ($HOMO_{-2}$–LUMO) orbital, its experimental and calculated band gaps are about 273 and 298 nm, respectively. The UV analysis was calculated at B3LYP/6-311++G(d,p) level, the electronic transition of (*E*)-2HBA3IPA is listed in Table 3. The recorded UV–Vis., spectra has shown in Fig. S3 (Supplementary) and the HOMO and LUMO plots of (*E*)-2HBA3IPA are shown in Fig. S4 (Supplementary).

Conclusions

In (*E*)-2HBA3IPA, an intra-molecular interaction is exist between hydroxyl hydrogen and nitrogen atom (O—H···N=C). Its calculated distance is about 1.725 Å in enol–imine closed form, whereas the enol–imine open form is not exist any such interaction between hydrogen and nitrogen. Due to the intra-molecular interaction the title molecule undergoes a little distortion by structurally and vibrationally. The band parameters calculated for enol–imine open form is show a slight deviation from open form. The experimental vibrational spectra are shows a very good agreement with theoretical wavenumber as well as spectra. Molecular hyperpolarizability is 8.5 times greater than urea, hence this title molecule possess considerable NLO property. The NBO analysis shows 101.84 kJ/mol during the intra-molecular hydrogen bond interaction, and also harvested the other intra-molecular hyperconjugative interaction. The less bond gap energy proposes the molecular reactivity.

Appendix A. Supplementary material

Supplementary data associated with this article can be found, in the online version, at http://dx.doi.org/10.1016/j.saa.2012.09.023.

References

[1] E. Hadjoudis, M. Vitterakis, M.I. Mavridis, Tetrahedron 43 (1987) 1345–1360.
[2] H. Ozisik, S. Saglam, S.H. Bayari, Sturct. Chem. 19 (2009) 41–50.
[3] J.V. Hidgon, B.W. Delage, R.H. Dashwood, Pharmacol. Res. 55 (3) (2007) 224.
[4] F. Billes, P.V. Podea, I. Mohammed-Ziegler, M. Tosa, H. Mikosch, D.F. Irimie, Spectrochim. Acta A 74 (2009) 1031–1045.
[5] L. Taiz, E. Zeiger, Plant Physiology, second ed., Sinauer Associates, Inc., Massachusetts, 1998.
[6] J.R. Carney, S.Z. Timothy, J. Phys. Chem. A 104 (2004) 8677–8688.
[7] P. Lissoni, R. Bucovec, A. Bonfonti, L. Giani, A. Mandelli, M.G. Roselli, F. Rovelli, L. Fumapalli, J. Pineal Res. 30 (2) (2001) 123.
[8] E.S. Howard, E.P. Burrows, M.J. Marks, R.D. Lynch, Fu-Mingchen, J. Am. Chem. Soc. 99 (1977) 707–713.
[9] Gaussian 03 program, (Gaussian Inc., Walling ford CT), 2004.
[10] H.B. Schlegel, J. Comput. Chem. 3 (1982) 214–218.
[11] G. Rauhut, P. Pulay, J. Phys. Chem. 99 (1995) 3093–3100.
[12] D. Michalska, Raint Program, Wroclaw University of Technology, 2003.
[13] D. Michalska, R. Wysokinski, Chem. Phys. Lett. 403 (2005) 211–217.
[14] H. Karabiyik, H. Petek, N.O. Iskeleli, C. Albayrak, Struct. Chem. 20 (2009) 1055–1065.
[15] H. Petek, C. Albayrak, M. Odabasoglu, I. Senel, O. Buyukgungor, Struct. Chem. 21 (2010) 681–690.
[16] H. Karabiyik, R. Sevincek, H. Petek, M. Aygün, J. Mol. Model. 17 (2011) 1295–1309.

[17] B. Kosar, C. Albayrak, M. Odabasoglu, O. Büyükgüngor, Crystallogr. Rep. 55 (2010) 1207–1210.
[18] A.D. Khalaji, A.N. Chermahini, K. Fejfarrova, M. Dusek, Struct. Chem. 21 (2010) 153–157.
[19] Y. Wang, Z. Yu, Y. Sun, Y. Wang, L. Lu, Spectrochim. Acta A 79 (2011) 1475–1482.
[20] A.R. Choudhury, T.N. Guru Row, Acta Crystallogr. E60 (2004) o1595–o1597.
[21] M.A. Palafox, Int. J. Quant. Chem. 77 (2000) 661–684.
[22] L.J. Bellamy, The Infrared Spectra of Complex Molecules, vol. 2, Chapman and Hall, London, 1980.
[23] S. Gunasekaran, S.R. Varadhan, K. Manoharan, Asian J. Phys. 2 (1993) 165.
[24] J. Mohan, Organic Spectroscopy Principle and Applications, second ed., Narosa Publishing House Pvt. Ltd., 2005. p. 75.
[25] S.W. Bunte, G.M. Jenson, K.L. McNesby, D.B. Goodin, C.F. Chabalowski, Niemien, S. Suhai, H.J. Jalkanen, Chem. Phys. 265 (2001) 13–25.
[26] K. Bahgat, A.G. Ragheb, Cent. Euro. J. Chem. 5 (2007) 201–220.
[27] D.N. Sathyanarayanan, Vibrational Spectroscopy – Theory and Applications, second ed., New Age International (P) Limited Publisher, New Delhi, 2004.
[28] B. Smith, Infrared Spectral Interpretation, A Systematic Approach, CRC Press, Washington, DC, 1999.
[29] R.M. Silverstein, F.X. Webster, Spectroscopic Identification of Organic Compounds, sixth ed., John wiley & Sons Inc., New York, 2003.
[30] D. Michalska, D.C. Bienko, A.J.A. Bienko, Z. Latajaka, J. Phy. Chem. 100 (1996) 1186.
[31] G. Varasanyi, Assignments of Vibrational Spectra of Seven Hundred Benzene Derivatives, vols. 1–2, Adam Hilger, 1974.
[32] I.D. Sadekov, Russ. Chem. Rev. 30 (1970) 179.
[33] I. Hubert Joe, G. Aruldhas, S. Anbukumar, P. Ramasamy, J. Cryst. Res. Technol. 29 (1994) 685–692.
[34] Y. Erdogdu, M. Tahir Güllüoğlu, Spectrochim. Acta A 74 (2009) 162–167.
[35] N. Sundaraganesan, B. Dominic Joshua, K. Sethu, Spectrochim. Acta A 66 (2007) 381–388.
[36] M. Selverstein, G.C. Basseler, C. Morill, Spectrometric Identification of Organic Compounds, Wiley, New York, 1981.
[37] S. Bayari, S. Saglam, H.F. Ustundag, Experimental and theoretical studies of the vibrational spectrum of 5-hydroxytryptamine, J. Mol. Struct. (Theochem.) 726 (2005) 225.
[38] T.D. Klots, W.B. Collier, Spectrochim. Acta A 51 (1995) 1291–1316.
[39] W.B. Collier, T.D. Klots, Spectrochim. Acta 51A (1995) 1255–1272.
[40] N. Sundaraganesan, H. Umamaheswari, J.B. Dominic, C. Meganathan, M. Ramalingam, J. Mol. Struct. – Theochem. 85 (2008) 84.
[41] G. Varasanyi, Assignments of Vibrational Spectra of Seven Hundred Benzene Derivatives, vols. 1–2, Adam Hilger, 1974.
[42] G. Socrates, Infrared and Raman Characteristic Group Frequencies Tables and Charts, third ed., Wiley, New york, 2001.
[43] V.K. Rastogi, M.P. Rajpoot, S.N. Sharma, Ind. J. Phys 58B (1984) 311.
[44] N.P.G. Roeges, A Guide to the Complete Interpretation of Infrared Spectra of Organic Structure, Wiley, New York, 1994.
[45] M. Barathes, G. De Nunzio, M. Ribet, Polarons or proton transfer in chains of peptide groups?, Synth Met. 76 (1996) 337.
[46] C.Y. Panicker, H.T. Varghese, D. Philip, H.I.S. Nogueira, K. Kastkova, Spectrochim. Acta A 67 (2007) 1313–1320.
[47] M. Ramalingam, M. Joccob, P. Venuvanlingam, N. Sundaraganesan, Spectrochim. Acta A 71 (2008) 996–1002.
[48] M.K. Subramanian, P.M. Anbarasan, S. Manimegalai, J. Raman Spectrosc. 40 (2009) 1657–1663.
[49] H. Ozisik, S. Saglam, S.H. Bayari, Struct. Chem. 19 (2008) 41–50.
[50] N.B. Colthup, L.H. Daly, S.E. Wiberly, Introduction to Infrared and Raman Spectroscopy, Academic Press, New York, 1990.
[51] C. Castiglioni, M. Del zoppo, P. Zuliani, G. Zerbi, Synth. Met. 74 (1995) 171–177.
[52] P. Zuliani, M. Del zoppo, C. Castiglioni, G. Zerbi, S.R. Marder, J.W. Perry, Chem. Phys. 103 (1995) 9935.
[53] M. Del zoppo, C. Castiglioni, G. Zerbi, Non-Linear Opt. 9 (1995) 73.
[54] M. Del zoppo, C. Castiglioni, P. Zuliani, A. Razelli, G. Zerbi, M. Blanchard-Desce, J. Appl. Polym. Sci. 70 (1998) 73.
[55] C. Ravikumar, I. Huber Joe, V.S. Jayakumar, Chem. Phys. Lett. 460 (2008) 552–558.
[56] A.E. Reed, F. Weinhold, J. Chem. Phys. 78 (1983) 4066–4073.
[57] A.E. Reed, F. Weinhold, J. Chem. Phys. 83 (1985) 1736–1740.
[58] A.E. Reed, R.B. Weinstock, F. Weinhold, J. Chem. Phys. 83 (1985) 735–746.
[59] J.P. Foster, F. Wienhold, J. Am. Chem. Soc. 102 (1980) 7211–7218.
[60] J. Chocholousova, V. Vladimir Spirko, P. Hobza, Phys. Chem. Chem. Phys. 6 (2004) 37–41.